

# ON CORRELATIONS AND FRACTAL CHARACTERISTICS OF TIME SERIES

Nikolay K. Vitanov<sup>1\*</sup>, Kenshi Sakai<sup>2</sup> and Elka D. Yankulova<sup>3</sup>

<sup>1</sup> Institute of Mechanics, Bulgarian Academy of Sciences, Akad. G. Bonchev Str., Bl. 4, 1113, Sofia, Bulgaria, e-mail: vitanov@imbm.bas.bg

<sup>2</sup> Tokyo University of Agriculture and Technology, 3-5-8, Saiwai-cho, Fuchu-shi, Tokyo, 183-8509, Japan, e-mail: ken@cc.tuat.ac.jp

<sup>3</sup> Faculty of Biology, "St. Kliment Okhridski" University of Sofia, 8, Dragan Tsankov Blvd., 1162 Sofia, Bulgaria, e-mail: eyankulova@yahoo.com

## Abstract

Correlation analysis is convenient and frequently used tool for investigation of time series from complex systems. Recently new methods such as the multifractal detrended fluctuation analysis (MFDFA) and the wavelet transform modulus maximum method (WTMM) have been developed. By means of these methods (i) we can investigate long-range correlations in time series and (ii) we can calculate fractal spectra of these time series. But opposite to the classical tool for correlation analysis - the autocorrelation function, the newly developed tools are not applicable to all kinds of time series. The inappropriate application of MFDFA or WTMM leads to wrong results and conclusions. In this article we discuss the opportunities and risks connected to the application of the MFDFA method to time series from a random number generator and to experimentally measured time series (i) for accelerations of an agricultural tractor and (ii) for the heartbeat activity of *Drosophila melanogaster*. Our main goal is to emphasize on what can be done and what can not be done by the MFDFA as tool for investigation of time series.

Key words: nonlinear time series analysis, fractals, Hurst exponent, Hölder exponent

---

\*corresponding author

## Abstract

Корелационният анализ е удобен и често използван инструмент за изследване на времеви редове от сложни системи. В последните години бяха развити нови методи за анализ на корелации като например мултифракталният флукуационен анализ (MF DFA) или методът на максимумите на модулите на wavelet-трансформацията (WTMM). Чрез тези методи (i) ние можем да изследваме корелациите с дълъг обseg във времеви редове и (ii) да изчисляваме фракталните спектри на величините, характеризиращи тези времеви редове. Но противно на случая с класическия инструмент за корелационен анализ - автокорелационната функция, гореспоменатите методи не са приложими за всякакви времеви редове, а безразборното им прилагане може да доведе до грешни резултати и заключения. В тази статия ние обсъждаме възможностите и рисковете, свързани с прилагането на MF DFA метода към времеви редове от един генератор на случайни числа и към експериментално измерени времеви редове от (i) ускорения на трактор и (ii) от сърдечната дейност на *Drosophila melanogaster*. Нашата главна цел е да подчертаем какво може и какво не може да се направи с MF DFA метода като инструмент за изследване на времеви редове.

# 1 Introduction

The investigation of correlation properties is one of the first tasks that a researcher of a time series has to perform. The classical tool for this is the autocorrelation function which can be calculated for stationary as well as for the nonstationary time series. The autocorrelation function reflects the behaviour of the time series. If for an example a time series is periodic its autocorrelation function is periodic too. For the most experimentally measured time series however the correlation function decays and in simple systems this decay in the most of the cases is exponential one. Opposite to this in numerous complex systems, which consist of many interacting subsystems, the correlations decay with power law and are called long-range because at large time scales the power law function is always large than the exponential function.

The properties of the long-range correlations can be investigated by means of two recently developed methods: WTMM and MFDFA. WTMM is based on the properties of the wavelets [1, 2, 3, 4] and it leads to excellent results when the recorded time series are long enough. For shorter time series (usually below  $10^6$  values) more convenient is the much simpler for implementation MFDFA method based on the scaling properties of the so called fluctuation function. Below we shall discuss what can be done and what can not be done by the MFDFA method when it is applied to different kinds of time series. We use two kinds of experimentally recorded time series (i) three short time series for the acceleration of an agricultural tractor working in different regimes and (ii) two time series for the heartbeat activity of *Drosophila melanogaster*. In addition we shall investigate a time series obtained by a random numbers generator in order to illustrate the monofractal properties of a time series.

The paper is organized as follows. In the next section we discuss some multifractal quantities and how they can be calculated by the MFDFA method. In section 3 we give more information about the time series and analyze their autocorrelation functions. In section 4 we analyze the time series by means of the MFDFA method. Several concluding remarks are summarized in the last section.

## 2 Generalized dimensions, fractal spectra, Hölder and Hurst exponents

Let us have a set  $S$  which lies in an  $N$ -dimensional Cartesian space covered by a grid of  $N$ -dimensional boxes of edge length  $\epsilon$ . Let  $\epsilon$  be small and we need  $N^*(\epsilon)$  boxes to cover our set. The box-counting dimension of the set is

$$(1) \quad D_0 = \lim_{\epsilon \rightarrow 0} \frac{\ln N^*(\epsilon)}{\ln(1/\epsilon)}$$

$D_0$  is not an integer for some sets. These sets are called fractals.  $D_0$  is a member of the spectrum of the  $D_q$  dimensions

$$(2) \quad D_q = \frac{1}{1-q} \lim_{\epsilon \rightarrow 0} \frac{\ln I(q, \epsilon)}{\ln(1/\epsilon)}$$

where  $q$  is a continuous index and  $I(q, \epsilon)$

$$(3) \quad I(q, \epsilon) = \sum_{k=1}^{N^*(\epsilon)} \mu_k^q,$$

is a sum over the  $N^*$  boxes of size  $\epsilon$  which cover the set.  $\mu_k$  is the natural measure i.e. it is a measure of the frequency with which typical orbit visit various boxes covering the attractor for the limit case when the length of the orbit goes to infinity (in addition the frequencies have to be the same for all initial conditions in the basin of attraction of the attractor except for a set with Lebesgue measure 0). Thus for  $\mu_k$  we have

$$(4) \quad \mu_k = \lim_{T \rightarrow \infty} \frac{\xi(c_k, \mathbf{x}_0, T)}{T},$$

where  $\xi$  is the time the orbit originating from  $\mathbf{x}_0$  spends in the cube  $c_k$  in the time interval  $0 \leq t \leq T$ . From (2) by means of the L'Hospital rule we easy can obtain

$$(5) \quad D_1 = \lim_{\epsilon \rightarrow 0} \frac{\sum_{k=1}^{N^*}(\epsilon) \mu_i \ln \mu_i}{\ln \epsilon}$$

$D_1$  is called also information dimension. In general  $D_0 \geq D_1 \geq D_2 \geq \dots$ . If  $D_q$  varies with  $q$  the measure, associated with  $D_q$  is called multifractal measure. The measure can have different behavior in each cube covering the set regardless of how small is its size  $\epsilon$ . Thus the dimension is not enough for a characterization of the measure and we need additional characteristic quantities. One such quantity is the coarse-grained Hölder exponent for each box

$$(6) \quad \alpha = \frac{\ln \mu(box)}{\ln \epsilon}$$

$\mu$  can have irregular behavior for different boxes. When the box size decrease and  $\mu$  has statistically the same irregular behavior the measure is called self-similar [9]. For large class of such measures  $\alpha$  lies between  $\alpha_{min} > 0$  and  $\alpha_{max} < \infty$ . For given  $\epsilon$  we can count the number  $N_\epsilon$  of the boxes with value of  $\alpha$  in small interval around a prescribed value. Thus we can define the coarse-grained spectrum

$$(7) \quad f_\epsilon(\alpha) \propto -\frac{\ln N_\epsilon(\alpha)}{\ln \epsilon}$$

From (7) we obtain  $N_\epsilon(\alpha) \approx \epsilon^{-f(\alpha)}$ , i.e. the relationship which has a form analogous to this one for the dimension above. Thus  $f(\alpha)$  can be treated as fractal dimension of the subsets  $S_\alpha$  of  $S$  having coarse grained Hölder exponent equal to  $\alpha$ . If  $f(\alpha)$  is not constant then for small  $\epsilon$  the set  $S$  is constructed by subsets  $S_\alpha$  of different dimensions  $f(\alpha)$ . Then the set  $S$  is called multifractal.

The multifractals can be characterized by different spectra. Below we shall obtain relationships for these spectra for the case  $\epsilon \rightarrow 0$ . We remember that the set  $S$  be covered by grid of boxes of unit size  $\epsilon$  and  $\mu$  is the probability measure on  $S$  ( $\mu(S) = 1$ ). Let  $\mu(c_k) = \mu_k$  where  $c_k$  denotes again the  $k$ -th cube. We have assigned a singularity measure  $\alpha_k$  to each cube

$$(8) \quad \mu_k = \epsilon^{\alpha_k}$$

For small  $\epsilon$  we can make continuous approximation for the number of cubes for which  $\alpha_k$  is between  $\alpha$  and  $\alpha + d\alpha$ , i.e., we can denote this number as

$$(9) \quad \rho(\alpha) \epsilon^{-f(\alpha)} d\alpha$$

By substitution of (8) in the relationship for  $I(q, \epsilon)$  and after a transition from a sum over the boxes to an integration over the  $\alpha$  we obtain

$$(10) \quad \begin{aligned} I(q, \epsilon) &= \sum_{k=1}^{N^*(\epsilon)} \epsilon^{\alpha_k q} = \int d\alpha^* \rho(\alpha^*) \epsilon^{-f(\alpha^*)} \epsilon^{q\alpha^*} = \\ &= \int d\alpha^* \rho(\alpha^*) \exp \{ [f(\alpha^*) - q\alpha^*] \ln(1/\epsilon) \} \end{aligned}$$

For small  $\epsilon$   $\ln(1/\epsilon)$  is large and the main contribution to the above integral is from the neighborhood of the maximum value of the  $f(\alpha^*) - q\alpha^*$ . Let  $f(\alpha^*)$  be smooth and the maximum is located at  $\alpha^* = \alpha(q)$  given by

$$(11) \quad \frac{d}{d\alpha^*} [f(\alpha^*) - q\alpha^*] |_{\alpha^*=\alpha(q)} = 0 \rightarrow \frac{df}{d\alpha^*} |_{\alpha^*=\alpha} = q$$

$$(12) \quad \frac{d^2}{d(\alpha^*)^2} [f(\alpha^*) - q\alpha^*] |_{\alpha^*=\alpha(q)} = 0 \rightarrow \frac{d^2 f}{d(\alpha^*)^2} |_{\alpha^*=\alpha} = q$$

Now we take the Taylor series representation of the function  $F(\alpha^*, q) = f(\alpha^*) - q\alpha^*$  around the point  $\alpha^* = \alpha(q)$  and substitute it in (10). The result is

$$(13) \quad \begin{aligned} I(q, \epsilon) &= \exp \{ [f(\alpha(q)) - q\alpha] \ln(1/\epsilon) \} \int d\alpha^* \rho(\alpha^*) \epsilon^{-(1/2)f''(\alpha(q))(\alpha^* - \alpha(q))^2} \\ &\approx \exp \{ [f(\alpha(q)) - q\alpha] \ln(1/\epsilon) \} \end{aligned}$$

Introducing (13) in (2) we obtain

$$(14) \quad D_q = \frac{1}{q-1} [q\alpha(q) - f(\alpha(q))]$$

From (11)

$$(15) \quad \frac{d}{dq} [(q-1)D_q] = \alpha(q) = \frac{d\tau}{dq}$$

Then

$$(16) \quad \tau(q) = (q-1)D_q \rightarrow D_q = \frac{\tau(q)}{q-1}$$

From (14)

$$(17) \quad f(\alpha(q)) = q \frac{d\tau}{dq} - (q-1)D_q = q \frac{d\tau}{dq} - \tau(q)$$

Thus for each  $q$  from (16) and (17) give  $\alpha(q)$  and  $f(\alpha)$  thus parametrically specifying the function  $f(\alpha)$ . The Hurst exponent sometimes is associated with the coarse-grained Hölder exponent for  $\epsilon \rightarrow 0$ . This can be done in the following way. For the cases in which the following relationship holds

$$(18) \quad \tau(q) = qh(q) - 1$$

we obtain

$$(19) \quad \alpha(q) = \frac{d\tau}{dq} = h(q) + q \frac{dh}{dq}$$

and

$$(20) \quad f(\alpha) = q\alpha - \tau(q) = q[\alpha - h(q)] + 1$$

But in which cases holds (18)? Let us consider stationary time series  $\{x_k\}, k = 1, \dots, N$  and let us use appropriate transformations in order to make all values positive and to normalize the time series, i.e.,

$$(21) \quad x_k \geq 0, \quad \sum_{k=1}^N x_k = 1$$

In this case we can associate the time series with some probabilities and we shall use this fact to derive (18). Let us construct the profile function for our normalized time series

$$(22) \quad Y_n = \sum_{k=1}^n (x_k - \langle x \rangle)$$

where  $\langle x \rangle$  is the mean of the time series. Now we divide the time series into  $N_s$  segments of length  $s$  and let for simplicity  $N_s = N/s$  is an integer. The sum

$$(23) \quad Y(\nu s) - Y((\nu - 1)s) = \sum_{k=(\nu-1)s+1}^{\nu s} (x_k - \langle x \rangle)$$

for the segment  $\nu$  is identical to the box probability  $p_s(\nu)$  which is the main building block of the corresponding partition sum  $Z_q(s)$  and scales with the  $\tau_q$  spectrum

$$(24) \quad Z_q(s) = \sum_{\nu=1}^{N/s} |p_s(\nu)|^q \propto s^{\tau(q)}$$

From other side for our time series  $\{x_k\}$  we can build a scaling function which contains the local Hurst exponent. This is the sum

$$(25) \quad \left\{ \frac{1}{2N_s} \sum_{\nu=1}^{2N_s} |Y(\nu s) - Y((\nu - 1)s)|^q \right\}^{1/q} \propto s^{h(q)}$$

From here we obtain

$$(26) \quad \frac{s}{2N_s} \sum_{\nu=1}^{2N/s} |Y(\nu s) - Y((\nu - 1)s)|^q \propto s^{qh(q)}$$

and finally

$$(27) \quad \sum_{\nu=1}^{N/s} |Y(\nu s) - Y((\nu - 1)s)|^q \propto s^{qh(q)-1}$$

A comparison of (24) and (27) leads to (18).

The implementation of the MFDFA method [5] follows the steps below. The starting point are our time series  $\{x_k\}$  of finite length  $N$ . First of all we have to determine the profile function. Here we have to mention the following. There are two possibilities. First of all we can use profile function as in (22), i.e.,

$$(28) \quad Y(i) = \sum_{k=1}^i (x_k - \langle x \rangle)$$

The final result of our analysis will be to obtain some values of the local Hurst exponent  $h$ . If we use (28) as profile function we can determine only positive Hurst exponents which are not quite close to 0. In all other cases we have to use as profile

$$(29) \quad \hat{Y}(i) = \sum_{k=1}^i (Y(k) - \langle Y \rangle)$$

where  $Y(k)$  comes from (28). Thus we shall obtain value of local Hurst exponent which is larger than the value of true exponent i.e.

$$(30) \quad \hat{h}(q) = 1 + h(q)$$

This is the final difference between the two branches of the method. We shall present here the first branch, which has the same steps as the second with the only difference that we have everywhere to change  $Y$  with  $\hat{Y}$  if we want to obtain the algorithm for the second branch. After the calculations of the profile function we have to divide it into segments of length  $s$ . As  $N/s$  in general is not an integer some part at the end of the time series will remain out of the  $N_s = \text{int}(N/s)$  segments. In order to incorporate the influence of this part into the analysis we divide the time series from the end to the beginning again to  $N_s$  segments of length  $s$ . Thus we obtain  $2N_s$  segments and for each segment calculate the local polynomial trend  $y_\nu(p)$ ,  $p = 1, \dots, s$ . The trend can be a polynomial of order  $m$ . Thus we perform MF DFA of order  $m$  and the coefficients of the polynom are obtained by a least-square fit of the corresponding segment. After the trend calculation we determine the variance

$$(31) \quad F^2(\nu, s) = \frac{1}{s} \sum_{i=1}^s \{Y[(\nu - 1)s + i] - y_\nu(i)\}^2$$

for the segments  $\nu = 1, 2, \dots, N_s$ . For the segments  $\nu = N_s + 1, N_s + 2, \dots, 2N_s$  the variance is

$$(32) \quad F^2(\nu, s) = \frac{1}{s} \sum_{i=1}^s \{Y[N - (\nu - N_s)s + i] - y_\nu(i)\}^2$$

The next step is an averaging over the segments for obtaining the  $q$ -th order fluctuation function ( $q$  is in general a real number). For  $q = 0$  the fluctuation function is

$$(33) \quad F_0(s) = \exp \left\{ \frac{1}{4N_s} \sum_{\nu=1}^{2N_s} \ln[F^2(\nu, s)] \right\}$$

and for  $q \neq 0$

$$(34) \quad F_q(s) = \left\{ \frac{1}{2N_s} \sum_{\nu=1}^{2N_s} [F^2(\nu, s)]^{q/2} \right\}^{1/q}$$

For large class of time series the fluctuation function has a power law behavior and from this power law for large  $s$  we can determine the local Hurst exponent

$$(35) \quad F_q(s) \propto s^{h(q)}$$

### 3 The time series and their autocorrelation functions

In order to achieve our goals we have selected time series from three different systems: an agricultural tractor, time series from the heartbeat activity of the classical object of Genetics - *Drosophila melanogaster* and a time series from a random number generator in order to illustrate the case of absence of correlations as well as the monofractal properties of some time series. The investigated time series are shown in Fig. 1. We investigate two kinds of experimental time series for acceleration of agricultural tractors. The time series from panels (a) and (b) of Fig. 1 are from experimental modeling of the bouncing phenomenon.

It arises when a machine travels on a rough road and consists of large-amplitude oscillations which can lead to injuries of the driver, to a lift of the machine (some times more than half-a-meter over the surface) and to damage of some of its elements. The time series for this phenomenon are recorded when the tractor moved on artificial rough road, consisting of 12 small kinks prepared on an asphalted surface. For this case we have several large amplitude oscillations when the tractor moves on the rough part of the road and in some time series we have also the noise background when the tractor moves on the smooth part of the road. Thus we can discuss these time series as time series of noise with superimposed periodic trend. The time series from panel (c) of Fig. 1 are recorded when the tractor has a construction exhibiting impact properties. This case has been chosen because the impact systems are frequent source of chaotic vibrations [6], [7]. The tractor has been converted to an impact system by adding vibrating subsoiler to it. The soil cutting chisel breaks a hard soil layer located at the depth between 30 and 50 cm from the field surface and it is oscillated in order to reduce the draft force and to improve the water infiltration into the soil. The oscillation is realized by a hydraulic power cylinder with two lift arms. This work mode is called ground-penetrating mode.

The time series in panels (d) and (e) of Fig. 1 are records of the heartbeat activity of *Drosophila melanogaster*. These flies are provided by Bloomington Drosophila Stock Center, U.S.A. The time series are ECGs (electrocardiogramms) for the first generation (the kids) obtained by male Dopa decarboxylase (Ddc) mutant (FBgn 0000422) located in chromosome 2, locus 37C1, crossed with female shibire (shi) (FBgn 0003392) located in chromosome 1, locus 13F7-12. Ddc codes for an enzyme necessary for the synthesis of four neurotransmitters: norepinephrine, dopamine, octopamine, serotonin, related to learning and memory. The shibire (shi) mutants cause paralysis at high temperature and eliminates the effect of the neurotransmitters on the heart. The ECGs have been recorded optically at a stage P1 (white puparium) of a *Drosophila* development when it is both immobile and transparent and the dorsal vessel is easily viewed. The object was placed on a glass slide in a drop of distilled water under a microscope (magnification 350 x). Fluctuation in light intensity due to movement of the dorsal vessel tissue was captured by photocells fitted to the one eyepiece of the microscope. The captured analogue signal was then digitized at 1 kHz sampling rate by data acquisition card and LabVIEW data capturing software supplied by National Instruments. Finally the time series from the random number generator are obtained by means of the generator `ran2` from [10]. In Fig. 2 are presented the autocorrelation functions for the investigated time series. The large amplitude oscillations in panels (a) and (b) reflect the bouncing phenomenon. The impact oscillations are clearly reflected by the almost periodic behaviour of the autocorrelation function in panel (c). The slowly decaying autocorrelations for the ECGs of *Drosophila* show some degree of anticorrelation at large  $n$ . Finally as it can be expected the time series from the random number generator are uncorrelated.

## 4 Fractal analysis of the time series

Excluding the time series from the random number generator which are uncorrelated, the other time series exhibit some degree of long range correlations. Below we shall discuss the question how far these correlations can be investigated by means of the modern methods such as the MFDFA. In order to answer this question we have to look at the fluctuation

functions connected to the time series. We shall calculate the fluctuation functions directly on the basis of the time series for the cases of tractor accelerations and for the time series from the random number generator. For the time series from *Drosophila* we first shall construct the time series for the intermaxima intervals (the time series for the time between two consequent maxima of the time series) and for the intermaxima time series we shall calculate the fluctuation functions and eventually the characteristic fractal quantities. The results are shown in Fig. 3. For the time series for the acceleration of the tractor in bouncing regime we can not apply the MFDFA method. The reason is that these time series (shown in panels (a) and (b) in Fig. 1) are too short and we can not divide them in large number of segments in order to have enough statistics for correct calculation of the fluctuation function. In order to apply the MFDFA the time series must have at least two thousand values. The minimum number of values - 4000 for which the fluctuation function is calculated here are the time series for the acceleration of the tractor in impact regime. The fluctuation function is not a straight line on a log-log scale - it has a kink as a reflection of periodicity of the time series. Thus these time series do not show scaling behaviour and we can not calculate the fractal spectra for them. On the other side we confirm the observation [8] that the periodic behaviour influences the fluctuation function. On panels (b) and (c) of Fig. 3 are presented the fluctuation functions for the intermaxima intervals of *Drosophila*. On panel (b) the fluctuation function is close to a straight line, i.e., the scaling properties can be assumed and the multifractal spectra can be calculated. Not so clear is the situation in panel (c). We shall carry further the calculations for this case in order to see how the not very large deviations from the scaling behaviour influence the form of the fractal spectra. The best scaling properties are exhibited by the time series from the random number generator - panel (d). This can be expected as these time series are specially selected for illustration of monofractal behaviour. Thus for calculation of the fractal characteristics from the initial 6 time series the requirements for length and presence of scaling properties have eliminated 3 time series. The  $h(q)$  spectra for the remaining three time series are presented in Fig. 4. The expected behaviour of such kind of spectrum is presented in panel (a) where  $h$  decreases with increasing  $q$ . This multifractal behaviour reflects the scaling properties of the time series as shown in panel (b) of Fig. 3. Multifractal behaviour is exhibited also by the second time series for the intermaxima intervals of *Drosophila melanogaster* shown in panel (b) of Fig. 4. As it can be seen from panel (c) of Fig. 4 for the time series from the random number generator  $h$  is a constant for all  $q$  which is characteristic feature for the monofractal behaviour.

Finally we calculate the  $f(\alpha)$  spectra. For the time series from the random number generator this spectrum is a point and it is not presented in Fig. 5. Panel (a) shows the spectrum for the time series with scaling properties shown in panel (b) of Fig. 3. The expected form for the  $f(\alpha)$  spectrum is parabolic one. This form is observed on panel (a) of Fig. 5. The maximum of the  $f(\alpha)$  spectrum shows at which  $\alpha$  is positioned the most statistically significant part of the time series, i.e., the subsets with maximum fractal dimension among all subsets of the time series. In our case  $f_{max} = 1$  at  $\alpha = 0.652$ . These and other characteristics of the  $f(\alpha)$  spectrum (such as its width at some value  $k f_{max}$ ,  $0 < k < 1$ ) can be used as tools for classification of time series with multifractal properties. The consequences of not fully scaling properties of the time series from panel (c) of Fig. 3 are observed in panel (b) of Fig. 5 where the parabolic form of the spectrum is slightly deformed. As such a form is different from the form for which we can make quantitative conclusions we can use such spectra only for qualitative conclusions and classifications. From the point

of view of genetics the different spectra correspond to the different genetic characteristics which the flies from the first generation obtained from the parents with different genetic heart defects. Thus only on the basis of the ECGs we can conclude that the two investigated *Drosophila* flies are affected in different way by the genetic defects of their parents. Thus the heartbeat dynamics of *Drosophila* is connected to its genetics. This conclusion opens the way for further intensive research on the relation between (i) the biomechanical properties of the heart of simple and more complex animals and humans and (ii) their genetic specifications.

## 5 Concluding remarks

In this paper we demonstrate the possibilities and risks when the multifractal detrended fluctuation analysis is applied to experimentally obtained time series. We have started with six time series from which only one was carefully selected in order to demonstrate monofractal and irregular behaviour. Then step by step we have demonstrated how the requirements of the method stop the investigation of different time series at different points as follows. The requirement for length was not satisfied by the time series for the acceleration of the tractor in bouncing regime. The investigation of the time series for the tractor acceleration in impact regime was stopped at the point where the requirement for scaling of the fluctuation function was imposed. At this point we allowed us to make a relative crude approximation for scaling properties of one of the time series for the heartbeat activity of *Drosophila*. The above crude approximation has the consequences in the multifractal spectra and especially in the  $f(\alpha)$  spectra. The monofractality of time series was clearly illustrated by the  $h(q)$  spectrum of the time series from the random number generator. Finally the  $f(\alpha)$  spectra have shown that the prescribed form of the spectrum for the multifractal behaviour can be assigned to only one of the six time series.

In conclusion we warn the researcher to be very careful when he or she applies the MF DFA to time series from real systems. Only small number of them are appropriate for such analysis. But when this analysis can be performed it can supply us with much quantitative and qualitative information about the relations between (i) the observed dynamics of the investigated complex system and (ii) the usually not visible processes, responsible for this dynamics.

## 6 Acknowledgments

N. K. V. gratefully acknowledges the support by NFSR of Republic of Bulgaria (contract MM 1201/02). K. S. thanks to the Japanese Society for Promotion of Science (JSPS) for the support by the Grant-in Aid for Scientific Research #09660269. E.D.Y. thanks the EC Marie Curie Fellowship Programm (contract QLK5-CT-2000-51155) for the support of her research.

## References

- [1] MUZY J. F., E. BACRY, A. ARNEODO. Wavelets and multifractal formalism for singular signals: application to turbulence data. *Phys. Rev. Lett.* **67** (1991), 3515-3518.

- [2] MUZY J. F., E. BACRY, A. ARNEODO. Multifractal formalism for fractal signals: The structure function approach versus the wavelet-transform modulus-maxima method. *Phys. Rev. E* **47** (1993), 875-884.
- [3] IVANOV P. CH., L. A. N. AMARAL, A. L. GOLDBERGER, S. HAVLIN, M. G. ROSENBLUM, Z. R. STRUZEK, H. E. STANLEY. Multifractality in human heartbeat dynamics. *Nature (London)*, **399** (1999), 461-465.
- [4] DIMITROVA Z. I., N. K. VITANOV. Chaotic pairwise competition. *Theoretical Population Biology* **66**(2004), 1-12.
- [5] KANTELHARDT J. W., S. A. ZSCHIEGNER, E. KOSCIELNY-BUNDE, S. HAVLIN S., BUNDE A., H. E. STANLEY. Multifractal detrended fluctuation analysis of nonstationary time series. *Physica A* **316** (2002), 87-114.
- [6] SAKAI K., K. AIHARA. Nonlinear vibrations in an agricultural implement system. *Int. J. Bif. Chaos*, **4** (1994), 465-470.
- [7] SAKAI K., K. AIHARA. Bifurcation structure of vibrations in an agricultural tractor-vibrating subsoiler system. *Int. J. Bif. Chaos* **10**, (1999), 2091-2098.
- [8] HU K., P. CH. IVANOV, Z. CHEN, P. CARPENA, H. E. STANLEY. Effect of trends on detrended fluctuation analysis. *Phys. Rev. E* **64** (2001), 011114.
- [9] EVERTS C. J. G., B.B. MANDELBROT in PEITGEN H. -O., H. JÜRGENS, D. SAUPE. *Chaos and Fractals. New Frontiers of Science*. Springer, New York (1992).
- [10] PRESS W. K., A. TEUKOLSKY, W. T. VETTERLING AND B. P. FLANNERY. *Numerical Recipes in Fortran. The Art of Scientific Computing*. Cambridge University Press, Cambridge (1992).

## FIGURE CAPTIONS

- Figure 1:  
The time series. Panels (a), (b), (c): time series for the acceleration of an agricultural tractor. Horizontal axis : time (unit for time is 8 ms for the panels (a) and (b) and 1 ms for the panel (c)). Vertical axis : accelerations (unit  $m/s^2$ ). Panels (d) and (e): characteristic time series for the heartbeat activity (ECG) of *Drosophila melanogaster*. Unit for time here is 1 ms. Panel (f): time series from the random number generator `ran2` [10]. This generator generates pseudorandom numbers in the interval  $[0,1]$ .
- Figure 2:  
Autocorrelation functions for the time series shown in Fig.1. Panels (a), (b): autocorrelations for the bouncing tractor. Panel (c): autocorrelations for a tractor working in impact regime. Panels (d), (e): autocorrelations for the heartbeat activity of *Drosophila melanogaster*. Panel (f): time series of pseudorandom numbers obtained by `ran2`.
- Figure3:  
Fluctuation functions (34). For all panels from bottom to the top the curves (marked with circles) are obtained for  $q = 2, 4, 6, 8$ . Solid line denote the r.m.s. power law fits of the corresponding curves. Panel (a): fluctuation functions for the time series of agricultural tractor in impact regime. Panels (b) and (c): fluctuation functions for intermaxima time series obtained by the time series of ECGs of *Drosophila melanogaster*. Panel (d): fluctuation function for the time series obtained by the generator `ran2`.
- Figure 4:  
Local Hurst exponent spectra  $h(q)$ . Panel (a):  $h(q)$  spectrum for the intermaxima time series obtained by the ECG time series of *Drosophila* shown in panel (d) of Fig.1. Panel (b):  $h(q)$  spectrum for the intermaxima time series obtained by the ECG time series of *Drosophila* shown in panel (e) of Fig. 1. Panel (c);  $h(q)$  spectrum for the time series obtained by the random number generator `ran2`.
- Figure 5:  
 $f(\alpha)$  spectra for the intermaxima time series obtained by the ECG of *Drosophila melanogaster*. Panel (a):  $f(\alpha)$  spectrum for the intermaxima time series obtained by the ECG of panel (d) of Fig. 1. Panel (b):  $f(\alpha)$  spectrum for the intermaxima time series obtained by the ECG of panel (e) of Fig. 1.

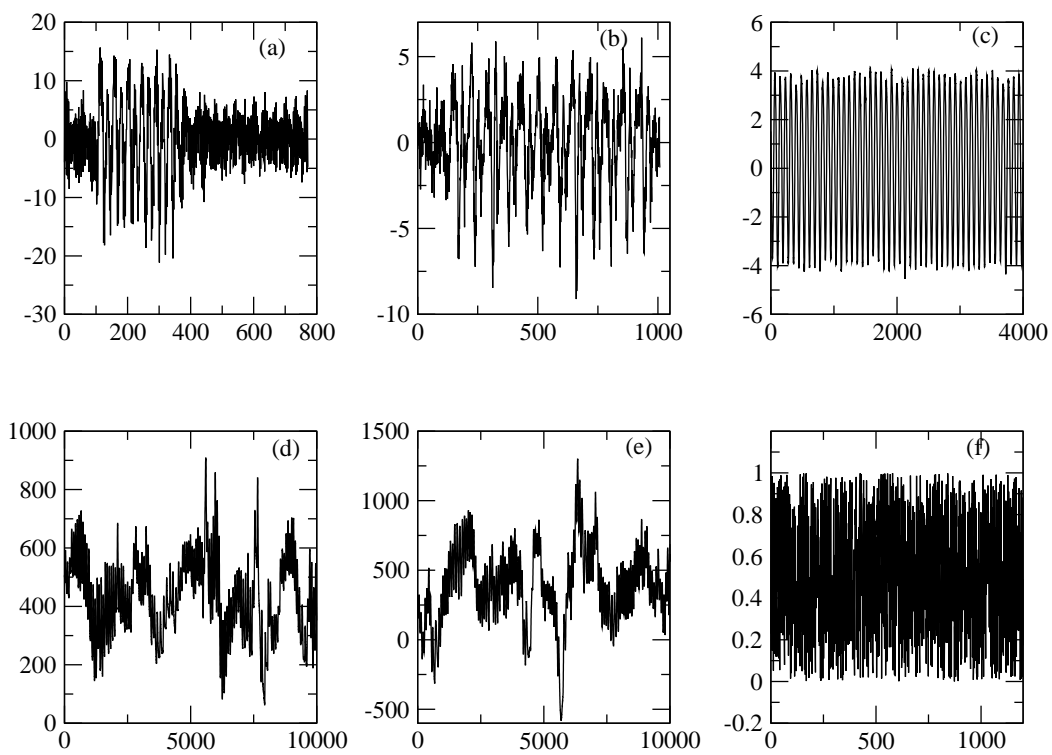


Fig. 1

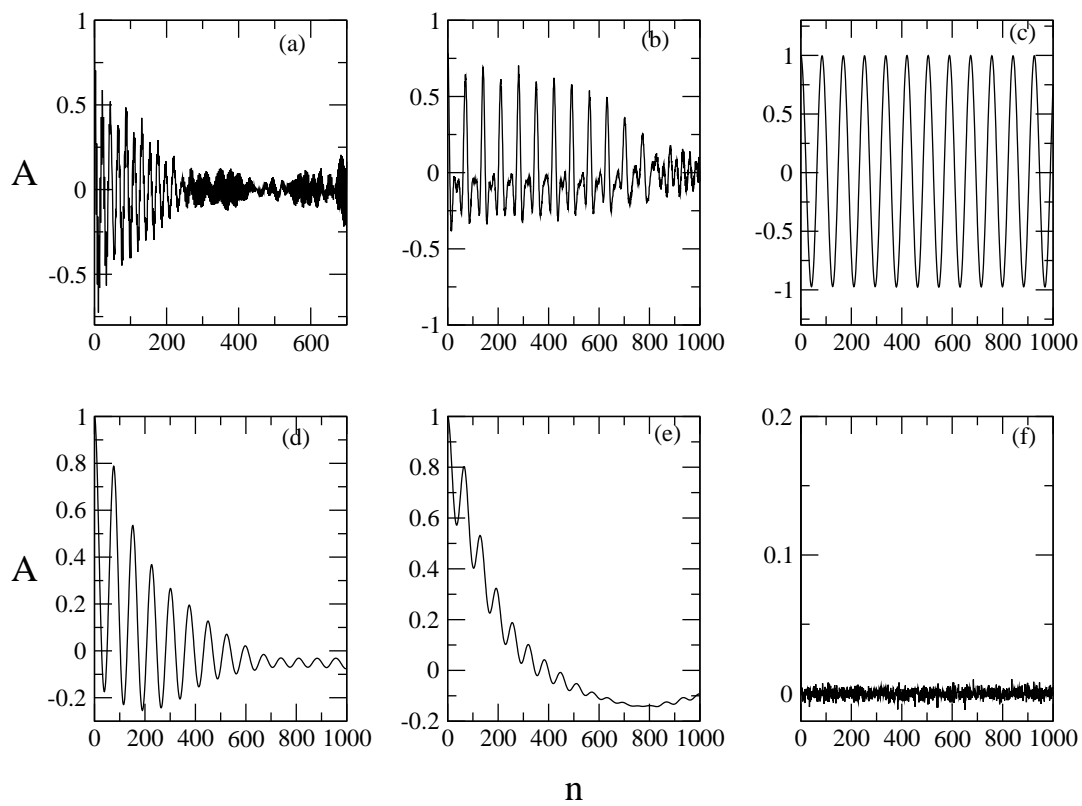


Fig. 2

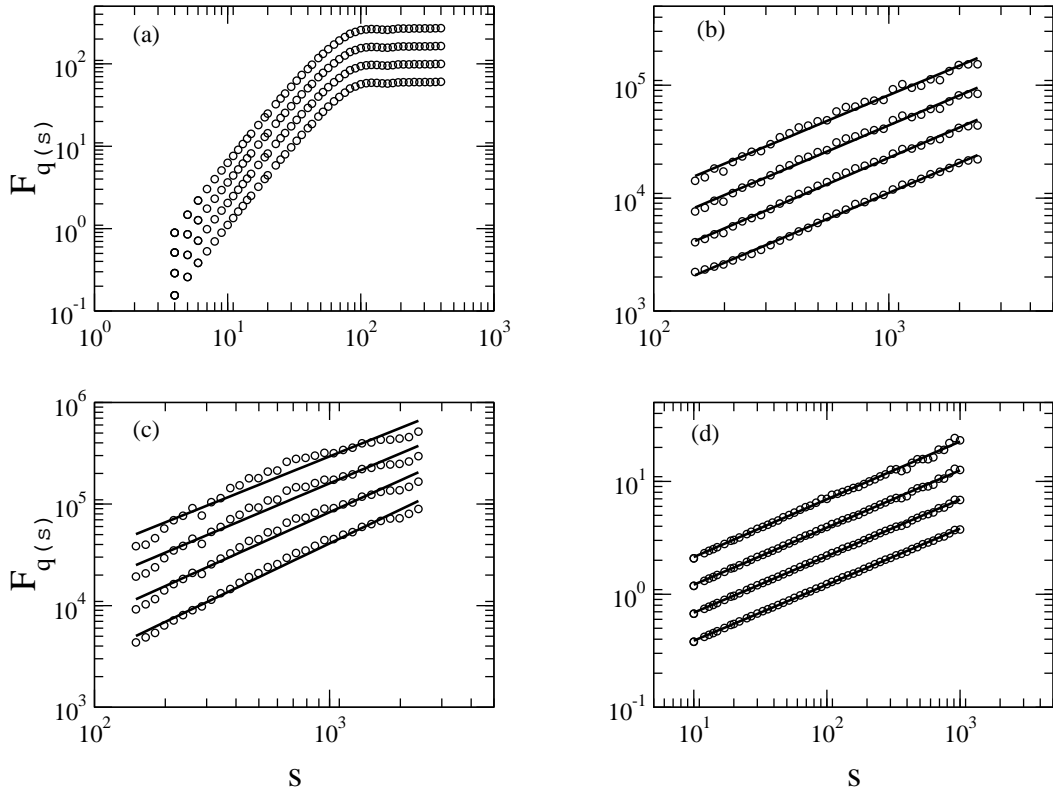


Fig. 3

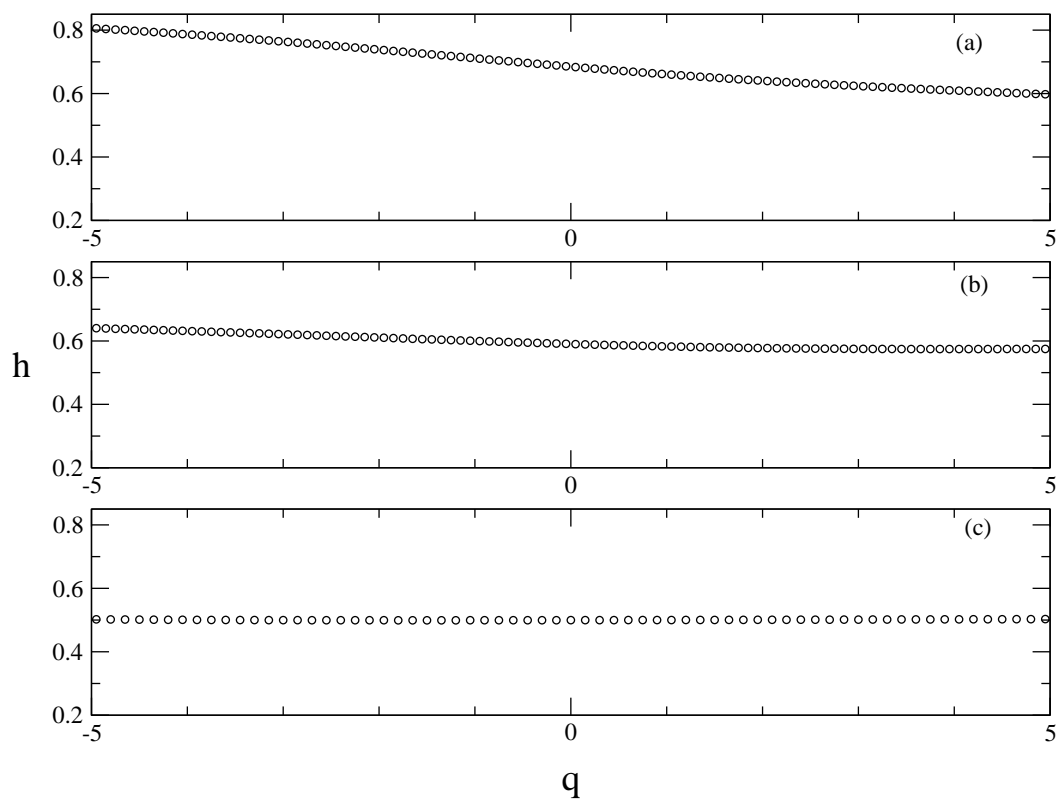


Fig. 4

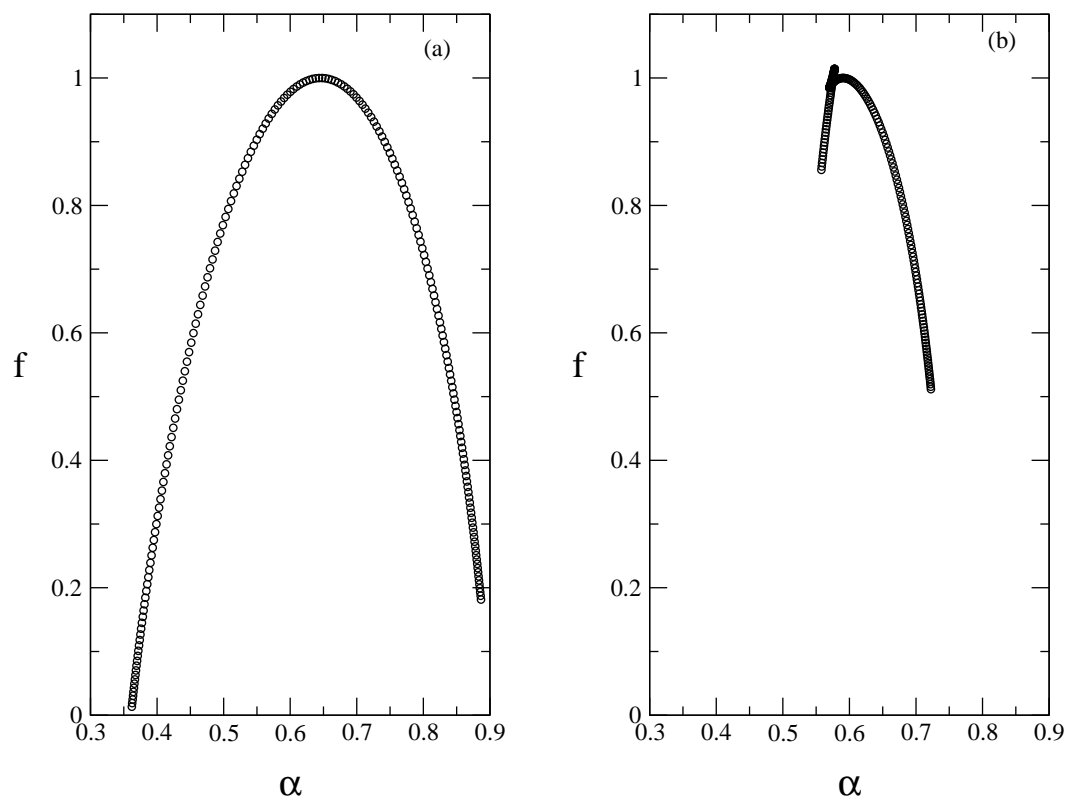


Fig. 5